

# Performance Assessment of Speed Controllers for Five-Phase PMSG with Integrated P&O MPPT algorithms Based Wind Energy Conversion Systems

Hossam H. H. Mousa<sup>1</sup>, Abdel-Raheem Youssef<sup>1</sup>, Essam E. M. Mohamed

<sup>1</sup>(Hossam H. H. Mousa  0000-0003-4753-2998)



**Abstract** To deal with the remarkable growth of global electricity demand, renewable energy sources (RESs), especially wind energy, are included in the power grid instead of the conventional generation stations which utilize fossil fuels to wipe out their serious influences on the environment such as the greenhouse effect. Hence, various control techniques are utilized on the wind energy conversion system (WECS) for adapting the generating wind power for accomplishing power grid requirements. During the integration of perturb and observe (P&O) maximum power point tracking (MPPT) algorithms, several drawbacks are investigated such as rotor speed fluctuations, and speed tracking loss. So, it is crucial to accurately design the speed controllers to overcome and curb these problems for achieving maximum wind power harvesting. Several speed controller types are employed to regulate the rotor speed with the actual wind speed. Therefore, this article investigates a comparative study and performance assessment of different speed controllers namely, PI, sliding mode control (SMC), integral sliding mode control (ISMC), and model predictive controller (MPC), to show the effectiveness of each one and their performance during the incorporation of P&O MPPT algorithms under the same operating conditions using the five-phase permanent magnet synchronous generators (PMSGs) based on the WECS. To authenticate the performance of the applied speed controllers, simulation results using various wind speed variations are carried out using Matlab/Simulink. The simulation results revealed that using predictive controllers is suitable for speed controller applications to solve other controllers' drawbacks during using the conventional P&O MPPT algorithm.

**Keywords:** (PI and SMC; ISMC; MPC; P&O MPPT algorithm; WECS).


## 1 Introduction

To cope with the significant rise in global electricity demand, renewable energy sources (RESs) are integrated into the power grid instead of the conventional generation stations which depend on fossil fuels to eradicate their serious impacts on the environment like global warming [1]. According to the expanded use of RESs, wind energy is a promised sort of energy that will record significant participation in the global energy demand by around 20% by 2030 [2].

Several control techniques are applied to the wind energy conversion system (WECS) for adapting the kinetic wind energy using the wind turbine (WT) to develop the electrical energy [3]. To keep the electrical energy proper for grid integration, various converter topologies are utilized such as the machine-side converter (MSC) and the grid-side converter (GSC) [4]. Hence, the general overall control scheme of WECS is presented in Fig. 1, which is mandatory to deal with the power grid obligations under variations of environmental conditions like wind speed.

Related to the wind stochastic nature, it is essential to indicate its operational regions contingent on the measured speed from the distributed anemometers around the WT [5]. So, the vertical-axis WT (VSWT) are widely applied which can obtain the maximum power without the fear of the WT vibration and mechanical stress. Hence, the active operating mode of WTs is restricted by cut-in ( $V_{cut-in}$ ) and cut-out ( $V_{cut-out}$ ) speeds to harvest all the available wind power. Generally, the operating regions of WT can be summarized as follows, shown in Fig. 2:

Received: 21 June 2022/ Accepted: 4 July 2022

 Hossam H. H. Mousa, [H.Herzallah@eng.svu.edu.eg](mailto:H.Herzallah@eng.svu.edu.eg), [Hossam.Herzallah7@gmail.com](mailto:Hossam.Herzallah7@gmail.com)

<sup>1</sup>. Department of Electrical Engineering, South Valley University, Qena, Egypt

- Regions 1 and 4: The WT is prevented to run for safety commitments.
- Region 2: The maximum power point tracking (MPPT) algorithms are employed to get the full wind power.
- Region 3: To reduce the mechanical hazards, pitch control is utilized to limit the generated power to the rated WT power.

With the increased development of the WECS, various kinds of electrical generators are extensively employed such as, squirrel-cage induction generators (SCIGs), the doubly-fed induction generators (DFIGs), and the synchronous generators (SGs). Currently, the implementation of the permanent magnet SGs (PMSGs) are extensively utilized owing to their advantages and boosted power density without the necessity of the DC excitation current and gearboxes. Several articles review different generators and power converters for WECS applications in [6-8]. In recent times, the applications of multi-phase PMSGs are grown dramatically for WECS applications because of low current ripples, enhanced fault-tolerant capability (FTC)... etc. [9]. Among them, the five-phase PMSGs are extensively employed for small-scale [10] or large-scale [11] WECSs.

In order to get the maximum wind power, MPPT algorithms are crucial to apply, which are divided into several categories in many published articles the categories [4, 12, 13]. MPPT algorithms can be clustered commonly into two main groups: the indirect power controller (IPC) and the direct power controller (DPC). Among the MPPT algorithms, the perturb and observe (P&O) or hill climbing search (HCS) algorithms are highly applied to optimize the wind power and to precisely operate in the maximum power point (MPP) [14]. By applying the perturbation principle of the P&O algorithms, it is essential to deal with the milestone challenges such as the instance speed variations,

especially in large steps, and power fluctuations which required specific management of speed controllers for perfect control operation [15, 16].

Hence, speed controllers are used for regulating the rotor speed with the measured wind speed with the improvement capability of the overall dynamic system performance. Consistent with the merits and demerits and the operation strategy, speed controllers can be classified as linear, nonlinear or predictive controllers [17]. Although conventional PI speed controllers are increasingly used as a consequence of their simple structure and design, difficult gains tuning, poor dynamic response with overshoot and high sensitivity towards unfamiliar exterior turbulences, decline both the dynamic performance and system efficiency [18]. For achieving high performance and robust dynamic response, sliding mode control (SMC) is applied as a nonlinear speed controller as a replacement for conventional PI controllers to treat the WECS uncertainties of the controlled variables [19, 20]. Hence, the sliding surface and the steady-state error problem can be handled by using the integral sliding mode control (ISMC), which employed the integral sliding surface [21]. While the high-order sliding mode controllers are verified for managing the chattering phenomenon and reaching phase stability challenges [22, 23].

Lately, predictive speed controllers have the ability to improve and forecast the WECS behaviour by eliminating the shortcomings of linear speed controllers which require accurate specification of several WECS parameters. During the rapid variations of the control variables, predictive controllers require extensive complex calculations and long computation time to implement the nonlinearities and constraints of the WECS model [17]. Among predictive controllers, the model predictive controller (MPC) is usually utilized for monitoring various controlled variables such as torque, speed, current...etc. Which can be

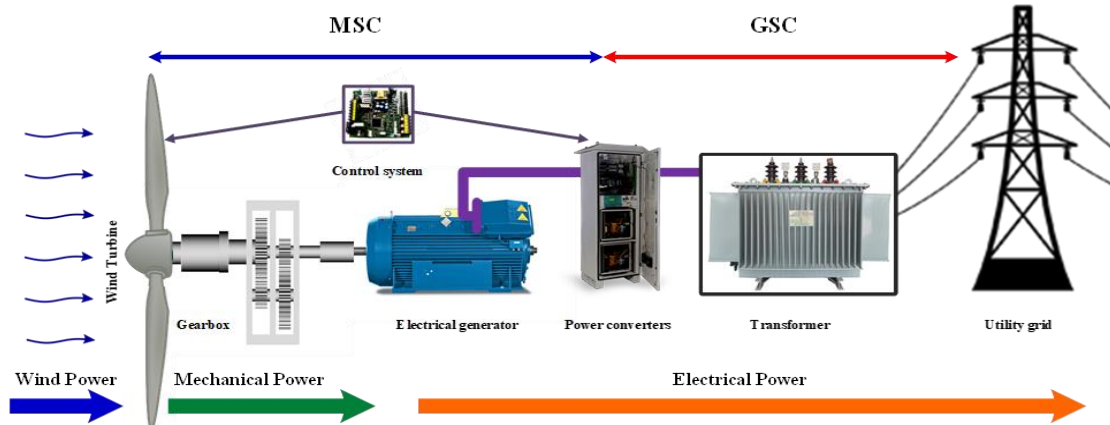


Fig. 1. Block diagram of a grid-tied WECS [12].

categorized into two major sorts of MPCs, continuous MPC and finite control set MPC. The continuous MPC (CMPC) requires a modulator to produce the inverter switching pulses for implemented parameters control. In stark contrast, the finite control set MPC (FCS-MPC) inclusively creates switching pulses [24].

In this article, the authors propose a comparative study and performance assessment of different speed controllers namely, PI, SMC, ISMC, and MPC, to show the effectiveness of each one and their performance during the incorporation of P&O MPPT algorithms under the same operating conditions using the five-phase PMSGs based on the WECS. The performance of the four-speed controllers is investigated under the step, ramp, and random wind speed variations and states their ability to overcome the speed oscillations which are produced from the P&O algorithms.

The rest of the article is structured as section 2 introduces the WECS modelling. An illustration of the P&O MPPT algorithm is discussed in section 3. While the explanation of the applied speed controllers is given in section 4, which follows the simulation results in section 5. The performance assessment of speed controllers is highlighted in section 6. Finally, a brief conclusion is demonstrated in the final.

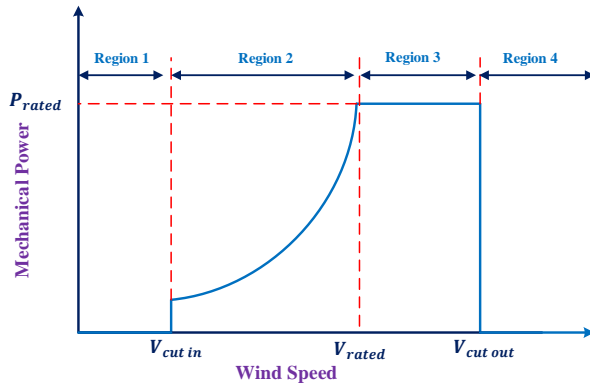


Fig. 2. WT operating regions.

## 2 WECS CONFIGURATION

To illustrate the WECS configuration, Fig. 3 shows mechanical, electrical, and miscellaneous components. The MSC involves WT, five-phase PMSG with MPPT, pitch, speed, and current controllers, which are responsible for extracting the wind power and converting it to electrical power. To tie the WECS with the satisfaction of the power grid requirements, the back-to-back converter (BTBC) with the DC-link is implemented. Both MSC and the GSC systems are discussed for the proposed WECS in detail in [25].

### 2.1 Wind Turbine Characteristics

To overcome the prior knowledge equations, several researchers investigate the WT aerodynamic modelling in [26]. Usually, the acquired mechanical power can be declared using the following equation which state for each operating region [27] in Eq. (1).

$$P_m = \begin{cases} 0, & V_{wind} \leq V_{cut\ in} \\ P_{rated} \left( \frac{V_{wind} - V_{cut\ in}}{V_{rated} - V_{cut\ in}} \right), & V_{cut\ in} \leq V_{wind} \leq V_{rated} \\ P_{rated}, & V_{rated} \leq V_{wind} \leq V_{cut\ out} \\ 0, & V_{cut\ out} \leq V_{wind} \end{cases} \quad (1)$$

In Regions 2, the WT is operated to enlarge the wind power under the variable wind speed, which is within the rated wind speed, by controlling the angle of attack of the WT blades. Hence, MPPT algorithms, such as P&O algorithms, are employed to adapt the shaft rotor speed with the actual wind speed to hunt the MPP in which the optimum amplitudes of tip speed ratio ( $\lambda_{opt}$ ) and power coefficient ( $C_{p,opt}$ ) that approach 8.1 and 0.48, respectively as noticed in Fig. 4(a) [5]. While in Region 3, the WT is forced to work and limit the output power to the rated power at high wind speed by pitch angle controllers for safety operation, as depicted in Fig. 4(b). Hence, the pitch angle is regularly modified as indicated by the following equation [28],

$$\beta_{ref} = \begin{cases} \beta_0 = 0, & 0 < \omega_m < \omega_{rated} \\ \frac{\Delta\beta}{\Delta\omega_m} (\omega_m - \omega_{rated}) + \beta_0, & \omega_m > \omega_{rated} \end{cases} \quad (2)$$

### 2.2 Multi-Phase PMSG Dynamic Model

According to their significant features, five-phase PMSGs are gradually utilized on the variable-speed WECSs. “The synchronous reference frame is employed to completely explain the operation of five-phase PMSG, such as stator voltage and torque equations, as analyzed in [11, 26, 29, 30]. The electromagnetic torque of five-phase PMSG is given as” [25],

$$T_e = \frac{5}{2} p \psi_1 i_{q1} \quad (3)$$

The mechanical torque is acknowledged as:

$$T_m = T_e + f \omega_m + J \frac{d\omega_m}{dt} = \frac{P_m}{\omega_m} \quad (4)$$

$$= \frac{1}{2} \rho \pi R^5 \frac{C_p(\lambda, \beta)}{\lambda^3} \omega_m^2$$

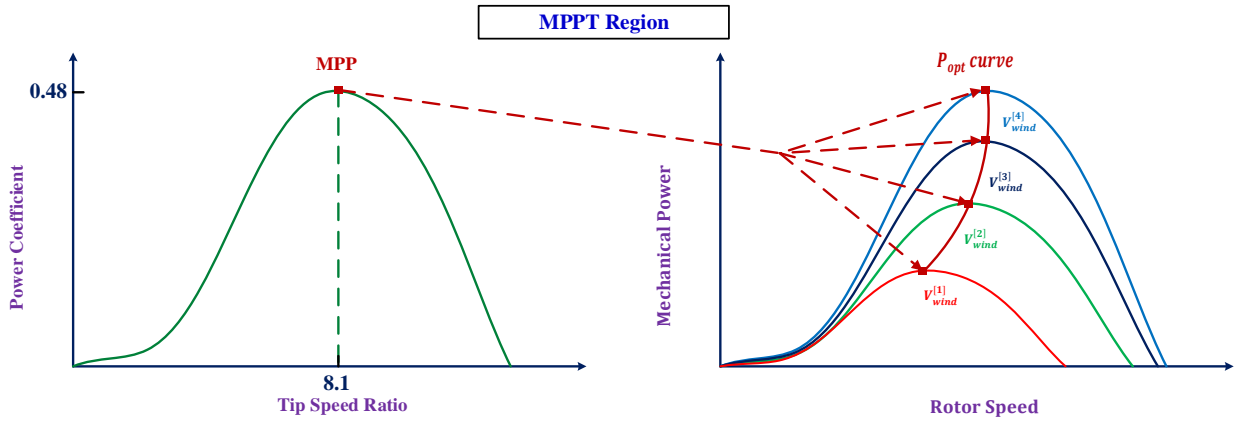
where  $f$  is the viscous damping coefficient and  $J$  is the total moment of inertia.

### 3 P&O Algorithms

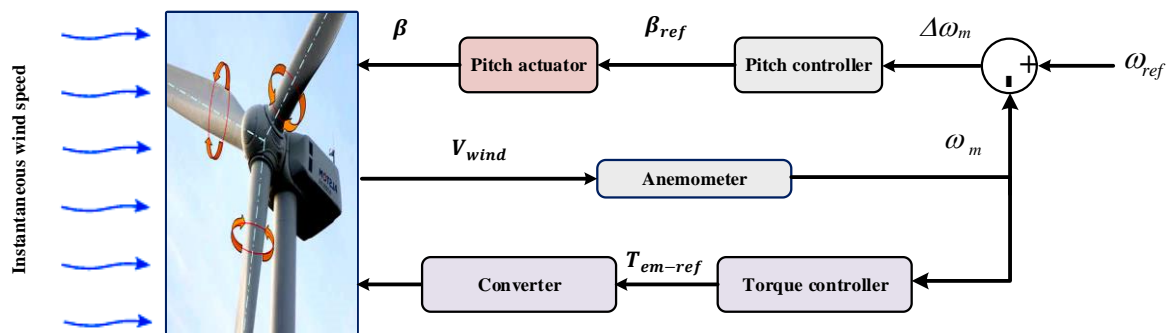
By perturbing the rotor speed with unique step-size and observing their impacts on the harvesting wind power to operate at the MPP, the P&O algorithms are suitable and efficient techniques to apply. In [12], the state of the art of P&O algorithms is investigated and classified in detail. Hence, to provide large speed fluctuations, the authors applied the conventional P&O (CPO) MPPT algorithm in [11] to extract the optimal power. Hence, Fig. 5 depicts the flow chart of the CPO algorithm [4].

### 4 Speed controllers

To specify the accurate MPP, the rotor speed should be in sync with the optimal speed created from the MPPT



(a) Characteristics of WT power under optimal values of  $\lambda_{opt}$  and  $C_{p,opt}$  [11].



(b) Block diagram of pitch angle controller [13].

algorithm via the outer speed control loop in the MSC as a reflection of the actual wind speed. Speed controllers, namely PI, SMC, ISMC, and MPC, are investigated and applied for five-phase PMSG as follows with a brief presentation to avoid information duplications.

#### 4.1 PI Speed Controller

The precise modelling of the PI controller using a detailed transfer function (TF), which declares the drive train dynamics as a function of  $(\omega_m, T_e)$  using a two-mass model, which is studied with detailed equations in [31]. In final, the general equation of the PI speed controller is  $PI_\omega(s) = k_{p(\omega)} + \frac{k_{i(\omega)}}{s}$ . “Here, the controller gains,  $k_{p(\omega)}$  and  $k_{i(\omega)}$ , are designed as  $k_{p(\omega)}/2(H_t + H_g) \ll \alpha_\omega$  and  $k_{i(\omega)}/k_{p(\omega)} \ll \alpha_\omega$ . The inner closed loop dynamics of the converter is neglected while the frequency range is  $\omega \ll \alpha_\omega$ . Thus, the speed closed loop TF as a function of  $\omega_{ref}$  and  $\omega_m$  is obtained from,

$$\frac{\omega_m}{\omega_{ref}} = \frac{2\zeta\omega_n s + \omega_n^2}{s^2 + 2\zeta\omega_n s + \omega_n^2} \quad (5)$$

Fig. 4. WT characteristics.

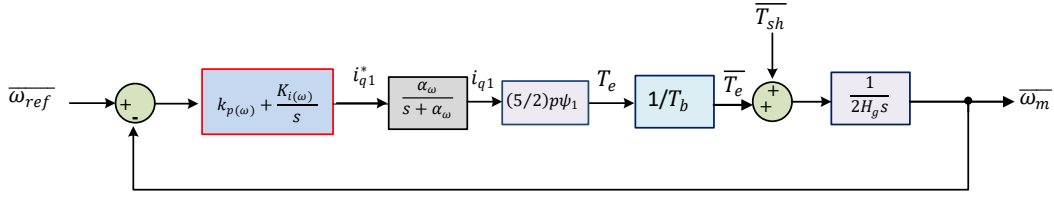


Fig. 6. Structure of the speed control loop.

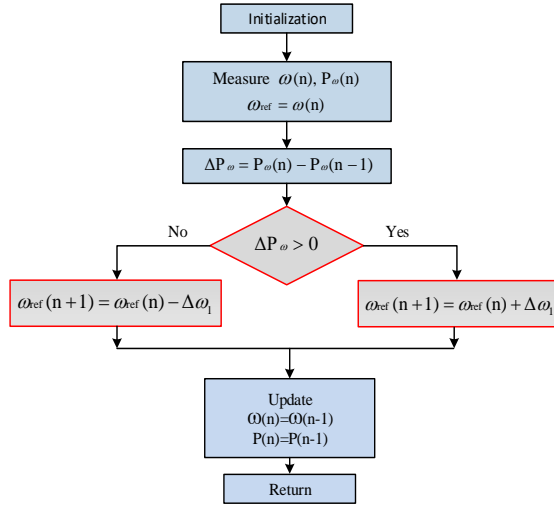


Fig. 5. Flow chart of the CPO algorithm.

Here,  $\zeta$  donates the speed controller damping ratio,  $\omega_n$  is the bandwidth of the closed-loop and  $\omega_n^2 = k \cdot \frac{k_i(\omega)}{2H_g}$ , in addition,  $2\zeta\omega_n = k \cdot \frac{k_p(\omega)}{2H_g}$ , where  $k = \frac{5}{2T_b} p\psi_{pm}$  [31]. The block diagram of the PI speed control scheme is portrayed in Fig.6

#### 4.2 Sliding Mode Speed Control strategy

In [23], the SMC strategy is discussed in detail to produce the final control effort equation as follows,

$$i_{q1}^* = \frac{2}{5} p\psi (T_m - J\dot{\omega}_{ref} - f\omega_m + K_\omega \text{sgn}(S_\omega)) \quad (6)$$

Where  $S_\omega$  is the sliding speed surface.

#### 4.3 Integral Sliding Mode Speed Control Strategy

By using the integration sliding surface for speed controller to overcome the drawbacks such as the slow response of the SMC as detailed in [3]. In final, ISMC solves the SMC problems by using the sat function as a

replacement of the sign function to minimize the chattering problem, also adding two terms for solving the reaching phase instability problem as shown in the following equation.

$$U^* = D^{-1} (-C - \rho_\omega \text{sat}(S_\omega) + K_c S_\omega + K_t \omega_m) \quad (7)$$

Where,  $U^* = i_{q1}^*$ ,  $\rho_\omega \geq |W|$ ,  $\text{sat}(S_\omega) = \frac{S_\omega}{|S_\omega|+1}$ ,  $D^{-1} = \left(\frac{2.5 K_p p\psi}{J}\right)^{-1}$

#### 4.4 Model Predictive Speed Control strategy

The MPC topology, the Single Input Single Output (SISO) system, is used to achieve the cost function in order to regulate and predict the rotor speed as shown in Fig. 7. In [31], the MPC tracks the rotor speed with its reference by using the following equations:

$$\omega_m(k+1) = \left(1 - \frac{f T_s}{J}\right) \omega_m(k) + \frac{T_s}{J} (T_m(k) - T_e(k)) \quad (8)$$

where  $T_s$  is the sampling time, then the cost function will be:

$$J_\omega = e_\omega([k+1|k])^T W e_\omega([k+1|k]) \quad (9)$$

where  $e_\omega([k+1|k])$  is one-step state error prediction and  $W$  is positive weighting matrix.

$$e_\omega([k+1|k]) = \omega_{ref} - \omega_m[k+1] \quad (10)$$

## 5 Simulation results

In this section, the simulation results are carried out using SMC for speed control and CPO algorithm as MPPT algorithm under rated wind speed, and pitch control during higher wind speed using the ramp and random wind speed profiles. The simulation results of the proposed WECS are verified with Matlab/Simulink. Furthermore, the MSC gains are designed and tuned as [11], the DC-link and GSC gains, and all controller's gains are set as given in [25].

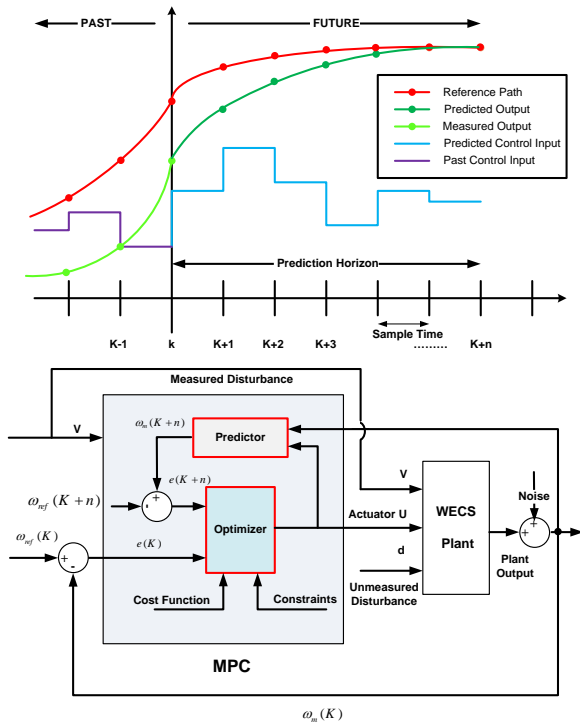


Fig. 7. Block diagram of MPC control scheme.

### 5.1 Ramp wind speed fluctuations

By using the ramp wind speed profile as shown in Fig. 8 (a), the pitch angle values, the TSR, and the  $C_p$  in Fig. 8 (b,c,d), respectively. It is observed that the pitch angle records zero degree and both optimal values of the TSR, and the  $C_p$  are achieved to gain the maximum available power from the wind. In stark contrast, it is clear that the pitch angle gradually rises to  $6^\circ$  and the TSR and the  $C_p$  are being declined to maintain the safe operation of the drive-train WECS during higher wind speed than the rated one. to keep the WT operating at rated power and the safe region at high speed. This, reflecting by the consequence of the rotor speed and the mechanical power which is depicted in Fig. 9 (a, b), respectively. According to the wind speed, both rotor speed and mechanical power track the reference at the MPPT region and restrict to the rated speed and power at the pitch control region. Furthermore, five-phase currents are given in Fig. 9 (c). On the other hand, it is obvious that the SMC can control the MSC for tracking the maximum power and in turn transfer it to the GSC. Hence, the performance effectiveness of the GSC variables is denoted in Fig. 10 such as the DC-link voltage, the phase voltage and the phase current, the real and reactive power, the d-q current components and the power factor. In general, the average DC-link voltage is maintained at 1150 V by using the DC-link control loop as shown in Fig. 10 (a), the phase voltage and phase current are operated at unity

power factor, as shown in Fig. 10 (b), which reflects on the injected power into the power grid. Fig.10 (c,d) show that both the real power and the d-axis current are regulated according to the references at each wind speed change, while reactive power and the q-axis current are being controlled to be zero in Fig.10 (c, e), respectively.

### 5.2 Random wind speed fluctuations

To confirm the effectiveness of the SMC for speed control during below and above rated wind speed, the random wind speed profile is applied with an average wind speed of 12 m/s and turbulence intensity equals 20%. Fig. 11 and Fig. 12 demonstrate the influence of the MPPT and the pitch control on the WT characteristics by applying SMC as a speed controller. Here, the MPPT algorithm provides the optimal  $C_{p,opt} = 0.48$  and  $\lambda_{opt} = 8.1$  under rated conditions, and the WT characteristics are limited to the rated values by the pitch control at high wind speed.

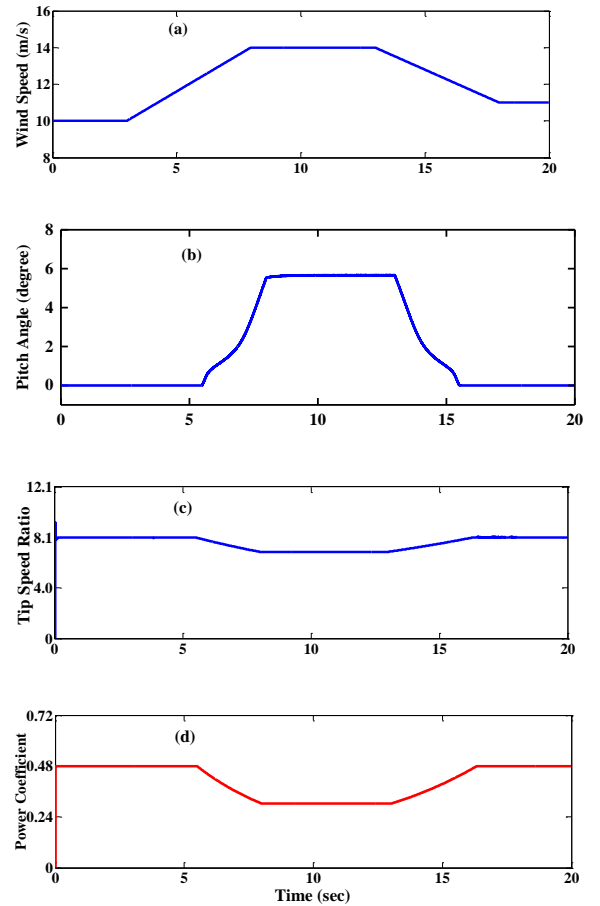
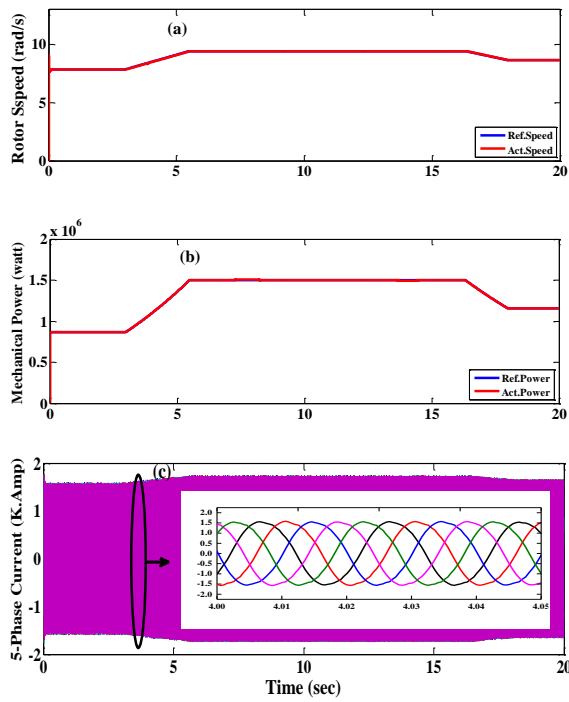
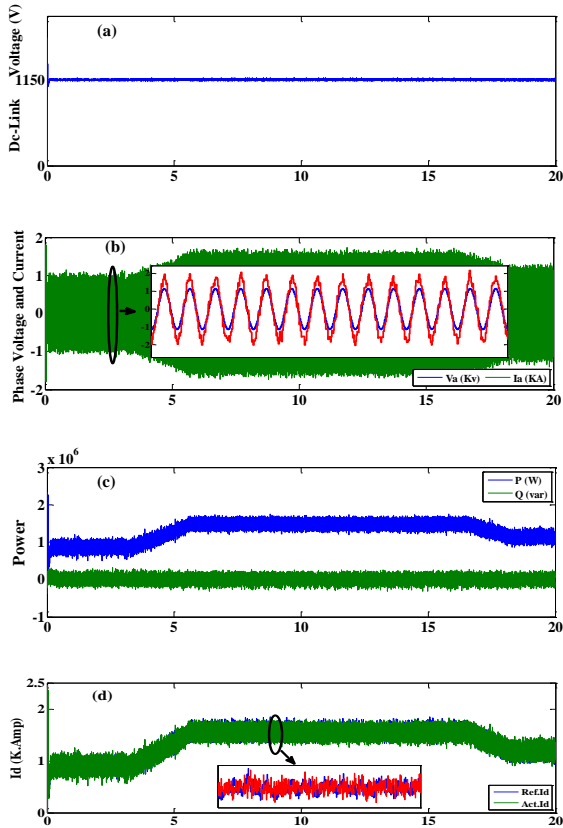


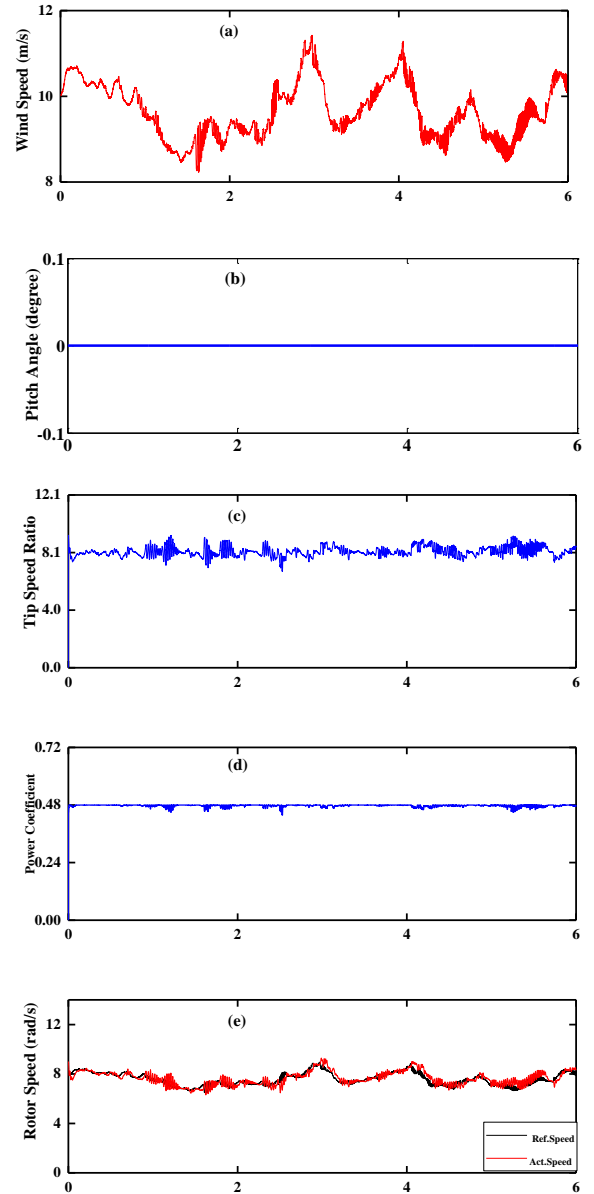
Fig. 8 (a) Wind speed (m/s) (b) Pitch angle (degree) (c) Tip Speed Ratio (d) Power coefficient



**Fig. 9** (a) Rotor speed (rad/s) (b) Mechanical power (MW) (c) 5-phase current (K.Amp)



**Fig. 10** (a)Dc-link voltage (b)Phase voltage and current (c) Grid power (d) Id (e) Iq



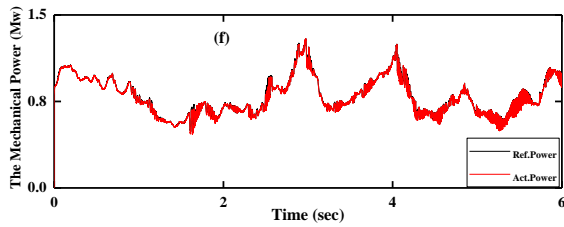


Fig. 11 the WT characteristic at the MPPT region

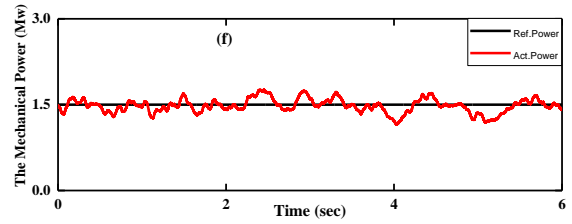
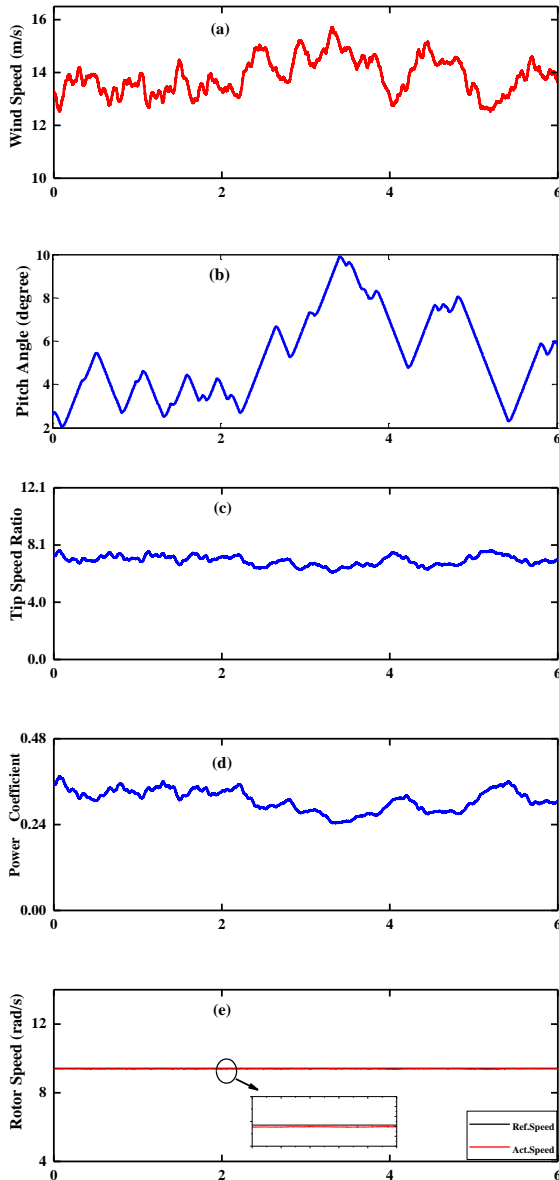


Fig. 12 the WT characteristic at the pitch control region



### 6 Performance assessment of speed controllers

To declare the performance assessment of speed controllers, namely PI, SMC, ISMC, and MPC, with integrated conventional P&O algorithm, this section significantly introduces a comparative study among them as shown in Fig. 13 and Table 1. It is obvious that the ISMC is used to deal with PI and SMC problems such as improving the sliding surface and overcoming the steady-state error and overshoot in response. Fig. 13 shows the simulation results of the PI, SMC, and ISMC in order to analyze each controller's performance. Hence, the simulation results show the superiority of ISMC over both PI and SMC which has the lowest steady-state error (0.204%) with settling time (122msec). The ISMC has the ability to cope with the reaching phase and chattering problems in the SMC case and slow response with an overshoot in the PI case. By summarizing the comparison details in Table 1, it is clear that the MPC accomplishes a slight performance improvement compared to other speed controllers such as steady-state error (0.167%) with settling time (97 msec). To conclude, using predictive controllers are suitable for speed controller applications to solve other controllers' drawbacks during using conventional P&O algorithm as MPPT algorithm.

TABLE I  
COMPARISON BETWEEN THE CONVENTIONAL PI, SMC, ISMC,  
AND MPC FOR WECS OVERTIME PERIOD (1 SEC)

Speed Controller	Steady-state error (Percentage %)	Settling time (msec.)
Conventional PI	0.841	952
SMC	0.675	207
ISMC	0.204	122
MPC [15]	0.167	97



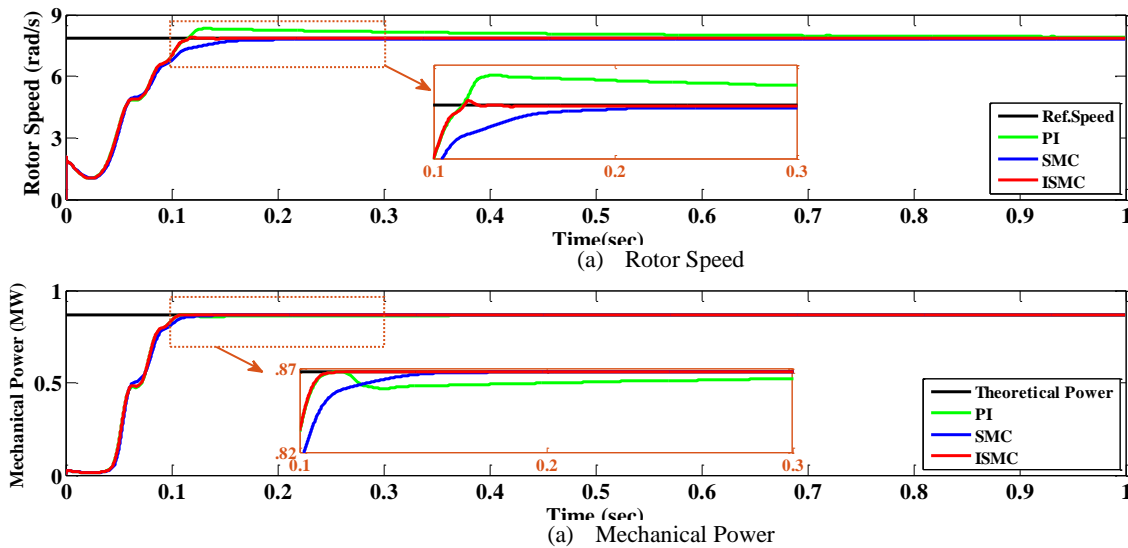


Fig. 13 comparison between conventional PI, SMC and ISMC for WECS

## 7 Conclusion

This article investigates a comparative study and performance assessment of different speed controllers namely, PI, SMC, ISMC, and MPC, to show the effectiveness of each one and their performance during the incorporation of P&O MPPT algorithms under the same operating conditions using the five-phase PMSGs based on the WECS. To authenticate the performance of the applied speed controllers and indicate their capability to overcome the speed oscillations, which are generated from the P&O algorithms, various wind speed variations, such as step, ramp, and random wind speed profiles, are used. The simulation results revealed that the MPC has perfect speed regulation and operation during wind speed variations compared to other speed controllers. To conclude, using predictive controllers are suitable for speed controller applications to solve other controllers' drawbacks during using conventional P&O algorithm as MPPT algorithm. The simulation results of the proposed WECS are carried out using Matlab/Simulink.

## References

- [1] J. Kaldellis and D. Apostolou, "Life cycle energy and carbon footprint of offshore wind energy. Comparison with onshore counterpart," *Renewable Energy*, vol. 108, pp. 72-84, 2017.
- [2] M. M. Hossain and M. H. Ali, "Future research directions for the wind turbine generator system," *Renewable and Sustainable energy reviews*, vol. 49, pp. 481-489, 2015.
- [3] H. H. Mousa, A.-R. Youssef, and E. E. Mohamed, "Optimal power extraction control schemes for five-phase PMSG based wind generation systems," *Engineering science and technology, an international journal*, 2019.
- [4] D. Kumar and K. Chatterjee, "A review of conventional and advanced MPPT algorithms for wind energy systems," *Renewable and Sustainable energy reviews*, vol. 55, pp. 957-970, 2016.
- [5] S. Tripathi, A. Tiwari, and D. Singh, "Grid-integrated permanent magnet synchronous generator based wind energy conversion systems: A technology review," *Renewable and Sustainable energy reviews*, vol. 51, pp. 1288-1305, 2015.
- [6] H. Li and Z. Chen, "Overview of different wind generator systems and their comparisons," *IET Renewable Power Generation*, vol. 2, no. 2, pp. 123-138, 2008.
- [7] Y. Zhao, C. Wei, Z. Zhang, and W. Qiao, "A review on position/speed sensorless control for permanent-magnet synchronous machine-based wind energy conversion systems," *IEEE Journal of Emerging and Selected Topics in Power Electronics*, vol. 1, no. 4, pp. 203-216, 2013.
- [8] M. Cheng and Y. Zhu, "The state of the art of wind energy conversion systems and technologies: A review," *Energy Conversion and Management*, vol. 88, pp. 332-347, 2014.
- [9] Mousa, Hossam HH, Abdel-Raheem Youssef, and Essam EM Mohamed. "Comparative Study of Fault-Tolerant Capability Performance for Three and Five-Phase PMSMs." *Journal of Control and Instrumentation Engineering E-issn (2019): 2582-3000*.
- [10] A.-R. Youssef, M. A. Sayed, and M. Abdel-Wahab, "MPPT Control Technique for Direct-Drive Five-Phase PMSG Wind Turbines with Wind Speed Estimation," *variations*, vol. 21, p. 22, 2015.
- [11] H. H. Mousa, A.-R. Youssef, and E. E. Mohamed, "Variable step size P&O MPPT algorithm for optimal power extraction of multi-phase PMSG based wind generation system," *International Journal of Electrical Power & Energy Systems*, vol. 108, pp. 218-231, 2019.
- [12] Mousa, Hossam HH, Abdel-Raheem Youssef, and Essam EM Mohamed. "State of the art perturb and observe MPPT algorithms based wind energy conversion systems: A technology review." *International Journal of Electrical Power & Energy Systems* 126 (2021): 106598.
- [13] H. H. H. Mousa, "Novel Perturb and Observe Techniques for Multi-phase PMSG Based Wind Generation System,

- <https://doi.org/10.13140/RG.2.2.29490.63689>," Department of Electrical Engineering, South Valley University 2020.
- [14] H. Ramadan, A.-R. Youssef, H. H. Mousa, and E. E. Mohamed, "An efficient variable-step P&O maximum power point tracking technique for grid-connected wind energy conversion system," *SN Applied Sciences*, vol. 1, no. 12, p. 1658, 2019.
- [15] H. H. Mousa, A.-R. Youssef, and E. E. Mohamed, "Model Predictive Speed Control of Five-Phase PMSG Based Variable Speed Wind Generation System," in 2018 Twentieth International Middle East Power Systems Conference (MEPCON), 2018, pp. 304-309: IEEE.
- [16] M. H. HH, A.-R. Youssef, and M. E. EM, "Improved Perturb and Observe MPPT Algorithm of Multi-Phase PMSG Based Wind Energy Conversion System," in 2019 21st International Middle East Power Systems Conference (MEPCON), 2019, pp. 97-102: IEEE.
- [17] H. Athari, M. Niroomand, and M. Ataei, "Review and classification of control systems in grid-tied inverters," *Renewable and Sustainable energy reviews*, vol. 72, pp. 1167-1176, 2017.
- [18] J. Zaragoza, C. S. Staines, A. Arias, J. Pou, E. Robles, and S. Ceballos, "Comparison of speed control strategies for maximum power tracking in a wind energy conversion system," in MELECON 2010-2010 15th IEEE Mediterranean Electrotechnical Conference, 2010, pp. 961-966: IEEE.
- [19] M. A. Sayed, A.-R. Youssef, M. N. Abdel-Wahab, and G. Shabib, "Sliding Mode Control of Variable Speed Wind Energy Conversion System Based on Five-Phase PMSG For MPPT," presented at the The 17th International Middle-East Power System Conference, Egypt, 2015.
- [20] E. Shehata, "A comparative study of current control schemes for a direct-driven PMSG wind energy generation system," *Electric Power Systems Research*, vol. 143, pp. 197-205, 2017.
- [21] R. Saravanakumar and D. Jena, "Validation of an integral sliding mode control for optimal control of a three blade variable speed variable pitch wind turbine," *International Journal of Electrical Power & Energy Systems*, vol. 69, pp. 421-429, 2015.
- [22] F. Valenciaga and P. Puleston, "High-order sliding control for a wind energy conversion system based on a permanent magnet synchronous generator," *IEEE transactions on energy conversion*, vol. 23, no. 3, pp. 860-867, 2008.
- [23] B. Yang et al., "Passivity-based sliding-mode control design for optimal power extraction of a PMSG based variable speed wind turbine," *Renewable Energy*, vol. 119, pp. 577-589, 2018.
- [24] Z. Zhang, C. Hackl, F. Wang, Z. Chen, and R. Kennel, "Encoderless model predictive control of back-to-back converter direct-drive permanent-magnet synchronous generator wind turbine systems," in *Power Electronics and Applications (EPE), 2013 15th European Conference on*, 2013, pp. 1-10: IEEE.
- [25] A.-R. Youssef, H. H. Mousa, and E. E. Mohamed, "Development of self-adaptive P&O MPPT algorithm for wind generation systems with concentrated search area," *Renewable Energy*, 2020.
- [26] H. H. Mousa, A.-R. Youssef, and E. E. Mohamed, "Hybrid and adaptive sectors P&O MPPT algorithm based wind generation system," *Renewable Energy*, vol. 145, pp. 1412-1429, 2020.
- [27] M.-A. Akbari, J. Aghaei, and M. Barani, "Convex probabilistic allocation of wind generation in smart distribution networks," *IET Renewable Power Generation*, vol. 11, no. 9, pp. 1211-1218, 2017.
- [28] R. Tiwari and N. R. Babu, "Recent developments of control strategies for wind energy conversion system," *Renewable and Sustainable energy reviews*, vol. 66, pp. 268-285, 2016.
- [29] L. Parsa, "Performance improvement of permanent magnet AC motors," Texas A&M University, 2005.
- [30] H. H. Mousa, A.-R. Youssef, and E. E. Mohamed, "Adaptive P&O MPPT algorithm based wind generation system using realistic wind fluctuations," *International Journal of Electrical Power & Energy Systems*, vol. 112, pp. 294-308, 2019.
- [31] H. H. Mousa, A. R. Youssef, and E. E. Mohamed, "Model predictive speed control of five - phase permanent magnet synchronous generator - based wind generation system via wind - speed estimation," *International Transactions on Electrical Energy Systems*, p. e2826, 2019.